Experimental investigation of pair dispersion with small initial separation in convective turbulent flows

Rui Ni (倪睿) and Ke-Qing Xia (夏克青)
Department of Physics, The Chinese University of Hong Kong, Shatin, Hong Kong, China
(Received 7 May 2012; published 12 June 2013)

We report an experimental investigation of pair dispersions in turbulent thermal convection with initial separation r_0 ranging from sub-Kolmogorov scale to scales in the inertial range. In the dissipative range of scales we observed the exponential growth of the separation between a pair of particles predicted by Batchelor and obtained a Batchelor constant 0.23 ± 0.07. For large r_0, it is found that, for almost all time ranges, both the mean-square separation and distance neighbor function exhibit the forms predicted by Batchelor, whereas the two quantities agree with Richardson's predictions for small r_0. Moreover, the measured value of the Richardson constant $g = 0.10 \pm 0.07$, which is smaller than those found in other turbulence systems. We also demonstrate the crossover of the mean-square separation from the exponential to the Batchelor regimes in both temporal and spatial scales.

DOI: 10.1103/PhysRevE.87.063006 PACS number(s): 47.27.tb, 44.25.+f, 47.55.pb

I. INTRODUCTION

A hallmark of turbulent flows is their ability to greatly enhance the mixing and dispersion of materials. A paradigm for investigating this phenomenon is the relative dispersion of a pair of particles, which is of central importance to a wide range of natural processes such as pollutants spreading in the atmosphere [1] and mixing in the oceans. While the above processes usually occur with particle separations in the inertial range of scales of the turbulent flows, an important regime of pair separation is in the very early stage where relevant spatial and temporal scales are within the dissipative subrange [2,3]. Turbulent dispersion and mixing in this regime is closely related to the reaction rate for fast-reacting scalars, such as in combustions and certain chemical reactions.

The concept of particle dispersion by turbulent flows was first introduced by Richardson, who attempted to explain the abnormally large observed value of turbulent diffusivity in the atmosphere. He introduced a quantity named the distance neighbor function (DNF) and the diffusion equation to describe the evolution of DNF [4]. With Kolmogorov's scaling theory, Obukhov refined Richardson's prediction and found that $\langle r^2 \rangle = g\epsilon t^3$, with r the pair separation, ϵ the mean kinetic energy dissipation rate, and g a dimensionless constant called the Richardson constant [5]. Batchelor [6], recognizing that over a short time the initial separation r_0 between the pair of particles would be important, obtained $\langle |\mathbf{r}(t) - \mathbf{r}_0|^2 \rangle = f(r_0)t^2$ for $\tau_\eta \ll t \ll t_0$, where $\tau_\eta = (\nu/\epsilon)^{1/2}$ is the Kolmogorov time scale and $t_0 = (r_0^2/\epsilon)^{1/3}$ is a characteristic time below which the initial separation is important. The Richardson-Obukhov scaling is now supposed to hold for $t_0 \ll t \ll t_L$, where t_L is the integral time scale. In the above $f(r_0) = [D_{LL}(r_0) + 2D_{NN}(r_0)]$, with D_{LL} and D_{NN} being the second-order longitudinal and transverse Eulerian structure functions, respectively.

It is clear that the above t^2 and t^3 power-law growth of pair separations (termed Batchelor and Richardson scalings, respectively) is relevant to dispersion and mixing processes in the inertial range of scales. For pair separations in the dissipative range, Batchelor was the first to argue that their growth rate should be proportional to the separation distance r itself [7], which leads to an exponential growth $\langle r^2 \rangle \sim r_0^2 \exp(\xi t)$ when both the initial and final particle separations are within the dissipative range, $r_0^2 \ll \langle r^2(t) \rangle \ll \eta^2$. Here the growth rate $\xi = 2B/\tau_\eta$ and B is called the Batchelor constant. However, in most previous experimental studies, the initial separation is in the inertial subrange [8,9]. As a result, the exponential growth regime has never been observed in experiments and the Batchelor constant has never been measured.

Recently, we have shown that the Lagrangian particle tracking velocimetry (PTV) can be applied to thermally driven turbulent flows and have obtained particle pairs with separations smaller than the Kolmogorov scale $\eta[=(\nu^3/\epsilon)^{1/4}]$ [10]. One advantage of the present system is that the range of its parameters is such that both the dissipative and inertial subranges can be accessed in the experiment. In fact, using PTV we have been able to accurately determine the energy dissipation rate ϵ from the measured dissipative range Eularian structure functions [11]. In this respect, turbulent thermal convection provides a good platform for studying properties of particle dispersions in both the dissipative and inertial subranges in a single experiment. From a different perspective, turbulent thermal convection, and buoyancy-driven turbulence in general, occurs ubiquitously in nature [12,13]. Therefore, studying two-particle dispersions in turbulent thermal convection is also important for understanding the transport and mixing of passive scalars in buoyancy-driven flows such as in the atmosphere and the oceans. However, buoyancy has been absent in most previous studies of pair dispersions in turbulent flows. In this paper, we report measurements of the mean-square separation $\langle \mathbf{r}^2(t) \rangle$ (and also $\langle |\mathbf{r}(t) - \mathbf{r}_0|^2 \rangle$) of a pair of particles in buoyancy-driven turbulent thermal convection.

II. EXPERIMENTAL SETUP AND METHODS

Lagrangian particle tracking velocimetry (PTV) was used in the experiments, which were carried out in a cylindrical cell with water as working fluid. The measurements were made in the cell center with r_0 ranging from dissipative to inertial range of scales. The height and diameter of the cell both equal to 19.2 cm, so the aspect ratio is one. The experiments were

conducted at a fixed Prandtl number $\mathrm{Pr} = \nu/\kappa = 4.4$ with various Rayleigh numbers $\mathrm{Ra} = \alpha g \Delta T H^3/\nu\kappa$ (from 2.9×10^9 to 1.3×10^{10}); here g is the gravitational acceleration, ΔT the temperature difference across the fluid layer, and α, ν, and κ, respectively the thermal expansion coefficient, kinematic viscosity, and thermal diffusivity of the working fluid. To compare the results with other turbulence systems, the microscale Reynolds numbers R_λ are determined by using $R_\lambda = \sqrt{15u'^4/\epsilon\nu}$ with u' the root-mean-square velocity and ϵ the energy dissipation rate in the cell center [10]. The tracking volume [$\delta V \simeq (5\ \mathrm{cm})^3$] in the center of the cell was illuminated by a laser beam, and the scattered light from the seeding particles (diameter $d_p = 50\ \mu$m polyamid, density $\rho = 1.03\ \mathrm{g/cm}^3$) was captured by three cameras simultaneously. The Stokes number $\mathrm{St} = \tau_p/\tau_\eta$ ranges from 10^{-4} to 10^{-3}, with τ_p being the time scale of the Stokes viscous drag due to interaction between particle and fluid. The number is much less than 1, indicating that the particles can be safely regarded as tracers. As the Kolmogorov time scale is $0.3 \sim 0.5$ s in the parameter range of our experiment and the camera frame rate is 50 or 100 fps depending on the Ra, the temporal resolution is sufficient to resolve dissipative range properties. The error of the particle position after calibration is $\sim 8\ \mu$m. However, due to the finite particle size and the diffraction effect, the minimum resolvable separation between a pair of particles is typically between 100 μm and 200 μm, which is less than $\eta \simeq 0.5$ mm in the experiment. Thus we are able to determine pair separations with initial separation r_0 smaller than the Kolmogorov length scale. In practice, we binned all pairs of particles with initial separation in the range $[r_0 - \delta r_0, r_0 + \delta r_0]$ when computing statistics. For $r_0 < 20\eta$, we take $\delta r_0 \approx \eta/5$ and for $r_0 \geqslant 20\eta$, $\delta r_0 \approx \eta$. Other details of the setup and calibration have been described elsewhere [10].

III. RESULTS AND DISCUSSION

Figure 1 plots in semilog scale four mean-square separations all with r_0 within the dissipative scale. It is seen that for $t < \tau_\eta$ and $r < 1.5\eta$ all curves with different Ra (R_λ) do follow an exponential growth as shown by the respective dashed lines. This initial exponential growth is observed for all nine values of Ra measured. From exponential fits we find no systematic Rayleigh (Reynolds) number dependency for the Batchelor constant, which leads to an average Batchelor constant $B = 0.23 \pm 0.07$. This number was first estimated by Batchelor and Townsend based on the assumption that the dissipative separation is mainly due to the stretching from the velocity gradient, which gives a range of $B = 0.35 \sim 0.41$ [14]. However, it was later argued that the original estimate is too large due to the lack of persistence of the rate-of-strain tensor and the role of vorticity [15] and it only serves as an upper limit. There are several simulation [15] and model [16] studies that attempt to estimate this constant and they gave $B = 0.093 \sim 0.13$. It is seen that our value of the Batchelor constant is larger than previous findings but still smaller than the upper limit proposed by Batchelor & Townsend [14].

Figure 2 shows the temporal evolution of $\langle |\mathbf{r}(t) - \mathbf{r}_0|^2 \rangle$ for different r_0, which increases, from bottom to top, from a dissipative range of scales to an inertial range of scales. The dotted and dashed lines in the figure show Batchelor and Richardson scalings, respectively. In PTV, the number of velocity pairs varies for different spatial separations, and pairs with the small separations generally have lower probability of being measured than those in some intermediate range of scales. Therefore, the one with smallest r_0 has the lowest number of particle pairs for statistics. In our experiment, there are 10^7 pairs of particles for $r_0 = 60.6\eta$, but only 10^3 for $r_0 = 0.9\eta$. In Fig. 2 we show only the statistical errors for $r_0 = 0.9\eta$, as the uncertainty for this initial separation is the biggest. One may note that even the largest error bar is within the symbol. For large r_0, there is a power-law regime in a range of time scales extending from 0.1 to 6 τ_η, whose exponent is very close to the one predicted by Batchelor [6], i.e., $\langle |\mathbf{r}(t) - \mathbf{r}_0|^2 \rangle \sim t^2$ (shown as the dotted line in the figure). It is seen that for those symbols with large initial separation and near the large end of t the exponent is slightly lower than 2 because those data are more likely to be affected by the finite measurement volume

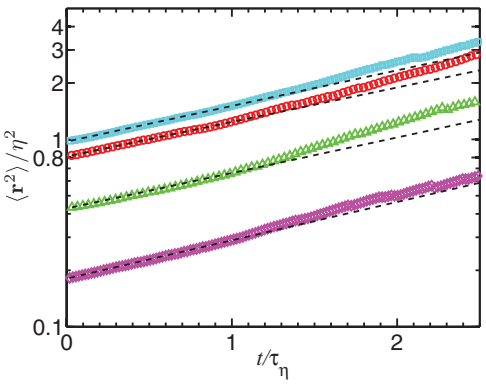

FIG. 1. (Color online) The mean square separation $\langle \mathbf{r}^2 \rangle$ as a function of time for four different Rayleigh numbers with initial separation smaller or close to η in a semilog plot. From top to bottom: Cyan squares ($\mathrm{Ra} = 1.0 \times 10^{10}$, $R_\lambda = 67$, $r_0 = \eta$); red circles ($\mathrm{Ra} = 1.3 \times 10^{10}$, $R_\lambda = 84$, $r_0 = 0.9\eta$); green triangles ($\mathrm{Ra} = 6.1 \times 10^9$, $R_\lambda = 53$, $r_0 = 0.7\eta$); pink diamonds ($\mathrm{Ra} = 2.9 \times 10^9$, $R_\lambda = 35$, $r_0 = 0.4\eta$). The dashed lines show the exponential fit to the respective data for $t \leqslant \tau_\eta$.

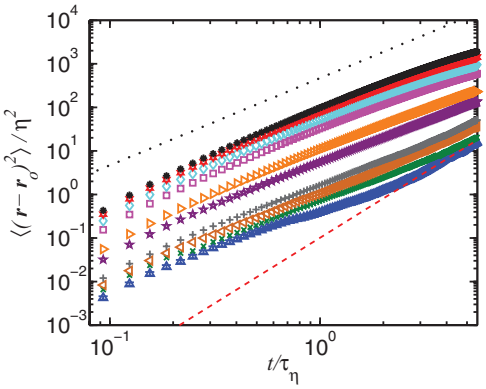

FIG. 2. (Color online) The normalized mean-square separation $\langle (\mathbf{r} - \mathbf{r_0})^2 \rangle / \eta^2$ as a function of time for different initial separations at $\mathrm{Ra} = 1.3 \times 10^{10}$ and $R_\lambda = 84$. From bottom to top: $r_0 = 0.9\eta$, 1.3η, 1.7η, 2.2η, 4.3η, 6.5η, 8.7η, 10.8η, 13.0η, 15.1η. The dotted line and dashed line indicate the Batchelor and Richardson regimes, respectively.

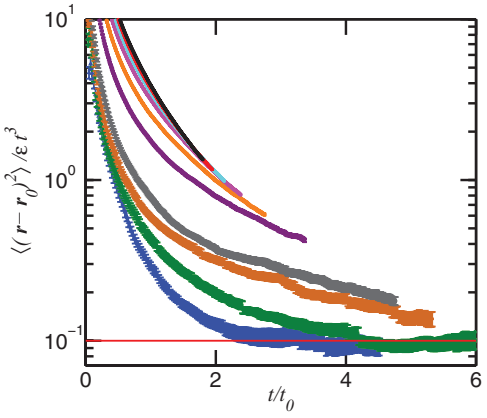

FIG. 3. (Color online) The mean-square separation compensated by t^3 with time normalized by t_0. The red solid line gives the Richardson constant $g = 0.1$. From bottom to top, the curves represent the same initial separations as those in Fig. 2. The thickness of each line at different times shows the uncertainties for the data.

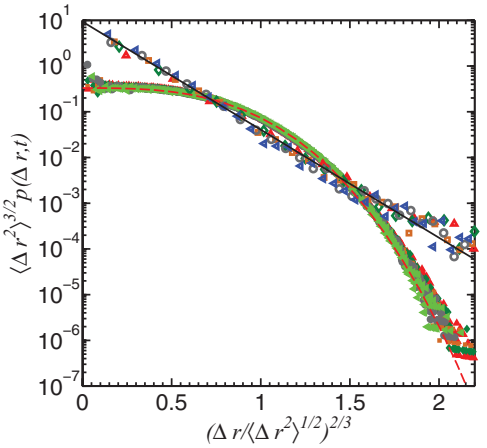

FIG. 4. (Color online) The distance neighbor functions for different initial separations at $\mathrm{Ra} = 1.3 \times 10^{10}$ ($R_\lambda = 84$). The red curved dashed line is Batchelor's predicted PDF and the black straight line is Richardson's. The open symbols show the experimental results for initial separation $r_0 = 0.9\eta$ with time t ranging from $3.1\tau_\eta$ to $5.5\tau_\eta$. The closed symbols show the results for initial separation $r_0 = 52\eta$ with time t ranging from $5.5\tau_\eta$ to $8.1\tau_\eta$.

effect [3,17]. For $r_0 = 0.9\eta$, there is no single power law for the entire range. For $t > 2\tau_\eta$ the behavior could be well described by the Richardson-Obukhov law for two-particle diffusion; i.e., $\langle |\mathbf{r}(t) - \mathbf{r}_0|^2 \rangle = g\epsilon t^3$. This can be seen more clearly in Fig. 3 as the plateau for the square separation compensated by Richardson-Obukhov scaling. Here it is seen that two data sets with the smallest initial separations ($r_0 = 0.9$ and 1.3η) reach the plateau, whereas the others show a similar trend towards the Richardson-Obukhov scaling but lack sufficient time to develop. This is consistent with the numerical simulation in the same thermal convection system [18]. Note that the time scale in Fig. 3 is normalized by a characteristic time $t_0 = (r_0^2/\epsilon)^{1/3}$, below which the initial separation is important.

From the red solid line we obtain the Richardson constant $g = 0.10 \pm 0.007$. Previous studies show that there is a large uncertainty on the value of g. For non-buoyancy-driven turbulent flows, more recent experimental and numerical studies [9,19–22] suggest $g \approx 0.5$. For thermal convection, a numerical study found that the value of g equals 0.16 and this smaller value was attributed to the correlated pair motion in thermal plumes [23]. As the plumes' motions are predominantly in the vertical direction, this would imply that pair dispersions should behave differently in different direction. However, by studying pair dispersion in the vertical and lateral directions separately we find the dispersion properties to be isotropic with the Richardson constant nearly the same in the vertical and the two lateral directions, i.e., each being 0.03. This suggests that pair dispersions in all directions are affected by some correlated motions. It is noted that flow in the cell center is affected by the large-scale circulation. This coherent motion is also azimuthally rotating, which may induce correlated motions in different directions.

The DNF represents the spherically averaged PDF for pairs of particles with separation r at time t, i.e., $p(r,t)$. Richardson first suggested that relative dispersion can be modeled by a diffusion equation for the DNF. For isotropic flow, the diffusion equation can be expressed as $\partial p(r,t)/\partial t = (1/r^2)\partial[r^2 K(r,t)\partial p(r,t)/\partial r]/\partial r$ with $K(r,t)$ being the diffusion constant. Richardson proposed that $K(r,t) \sim r^{4/3}$ based on experimental measurements in the atmosphere and, based on dimensional argument, Obukhov later suggested $K(r,t) = k_0\epsilon^{1/3}r^{4/3}$. This led to the solution $p_R(r,t) = \sqrt{143/2} \times 429/70(\pi\langle r^2 \rangle)^{-3/2} \exp[-(1287r^2/8\langle r^2 \rangle)^{1/3}]$. Assuming $K(r,t) \sim t^2$, Batchelor found another solution to the diffusion equation; i.e., $p_B(r,t) = (2\pi\langle r^2 \rangle/3)^{-3/2} \exp[-3r^2/2\langle r^2 \rangle]$. The two solutions are shown in Fig. 4 as a black solid line (Richardson's prediction) and red dashed line (Batchelor's prediction). In both solutions, the separation between two particles was assumed to be zero at the very beginning. Experimentally, however, even if one could resolve sub-Kolmogorov scale, the initial separation would be much larger than 0. One way to solve this problem is by subtracting all particle separations with their initial value, i.e., $\Delta r = r - r_0$, and replacing $p(r,t)$ with $p(\Delta r,t)$ [8]. In Fig. 4, the open symbols all have $r_0 = 0.9\eta$ and closed ones $r_0 = 52\eta$. There are five data sets at different times for each initial separation. The times are chosen to fall into the time range where the particle separations increase as t^2 ($r_0 = 52\eta$) and t^3 ($r_0 = 0.9\eta$) scalings, respectively. It is clear that the DNF results agree with Richardson's prediction for small r_0 and agree with Batchelor's prediction for large r_0.

To take a closer look at the Batchelor scaling, we show in Fig. 5 the mean-square pair separation compensated by $f(r_0)t^2$. Note that because the initial separation r_0 in our experiments varies continuously from the dissipative range to inertial range, we use the full function $f(r_0) = D_{LL}(r_0) + 2D_{NN}(r_0)$ for the coefficient of the Batchelor scaling, instead of its dissipative range ($\frac{1}{3}r_0^2/\eta^2$) or inertial range ($\frac{11}{3}Cr_0^{2/3}/\eta^{2/3}$) scalings as in some previous studies. It is seen from the figure that curves for all initial separations and for t from τ_η to $3\tau_\eta$ collapse onto one horizontal line with the height very close to unity. In the above the values of the Eulerian structure functions $f(r_0)$ were independently obtained from the measured particle trajectories [11], which

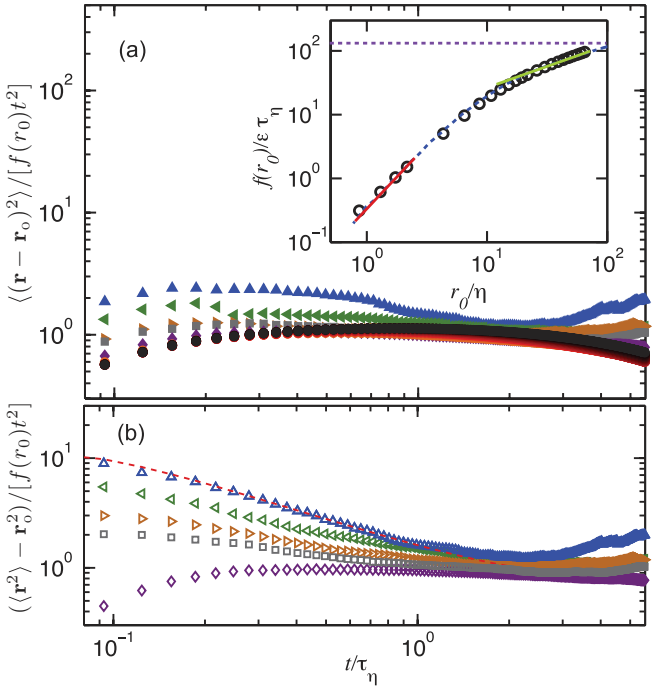

FIG. 5. (Color online) (a) The mean-square separation $\langle(\mathbf{r}-\mathbf{r}_0)^2\rangle$ compensated by $f(r_0)t^2$ as a function of normalized time t/τ_η for different initial separations measured at Ra $= 1.3\times10^{10}$ ($R_\lambda = 84$). From top to bottom: $r_0 = 0.9\eta$ (▲), $1.3\,\eta$ (◀), $1.7\,\eta$ (▶), 2.2η (■), 4.3η (♦). There are 18 data sets with $r_0 = 6.5\eta \sim 65\eta$ that collapse onto each other, which are represented by the solid circles. Inset: The black circles represent the values of $\langle(\mathbf{r}-\mathbf{r}_0)^2\rangle/t^2$ at $t = 2\tau_\eta$ for different r_0 and the blue dashed line that goes through all the symbols represents $f(r_0)$ determined from Eulerian structure functions. Both quantities are normalized by $\epsilon\tau_\eta$. The red (near the lower left corner) and green (near the upper right corner) solid lines are respectively $f(r_0) = \frac{1}{3}r_0^2/\eta^2$ and $f(r_0) = \frac{11}{3}Cr_0^{2/3}/\eta^{2/3}$ ($C = 1.56$ is the Kolmogorov constant [24]), which are the dissipative and inertial range scaling predictions for $f(r_0)$. The (horizontal) purple dashed line shows the large r_0 limit of $f(r_0) = 6R_\lambda/\sqrt{15}$. (b) $[\langle\mathbf{r}^2(t)\rangle - \mathbf{r}_0^2]/f(r_0)t^2$ vs t/τ_η. The open symbols here correspond to the closed ones in (a). The red dashed line shows $\{r_0^2\exp[0.42(t/\tau_\eta)] - r_0^2\}/f(r_0)t^2$ with $r_0 = 0.9\eta$.

are also shown as the dashed blue line in the inset of the figure. The values of $f(r_0)$ can also be obtained as the plateau heights of the compensated plots $\langle|\mathbf{r}(t)-\mathbf{r}_0|^2\rangle/t^2$ for various values of r_0 (not shown here), which are shown as the circles in the inset. It is seen that there is an excellent agreement between the values of the $f(r_0)$ obtained from the measured mean-square pair dispersion and the Bachelor scaling and those obtained directly from Eulerian structure functions. Also shown in the inset are the K41 predictions for the dissipative (red line), inertial range (green line), and the large-r_0 limit $6R_\lambda/\sqrt{15}$ (purple dashed line) of $f(r_0)$ [22]. The excellent collapse between circles and three solid lines indicates that the dispersion in the intermediate time domain is mainly controlled by the initial velocity difference between two particles with their separation extending from dissipative to inertial ranges. In Fig. 5(a) it is seen that the compensated $\langle|\mathbf{r}(t)-\mathbf{r}_0|^2\rangle$ for $r_0 \sim \eta$ and $t < \tau_\eta$ increases systematically as r_0 decreases. The reason is as follows. For very small t and $r_0 \lesssim \eta$ (so the velocity difference between the pair is very small), $\mathbf{r}(t)$ is not much different from $\mathbf{r}_0$ and their difference essentially represents random measurement errors. But because of the square, these errors do not cancel but add up after averaging over different pairs.

So far we have shown that our measured pair dispersions exhibit exponential growth in the dissipative range and power-law growth in the inertial range. However, these are manifested in different quantities, i.e., in $\langle r^2(t)\rangle$ and $\langle[\mathbf{r}(t)-\mathbf{r}_0]^2\rangle$, respectively. But in fact the pictures are consistent and there exists a crossover between the two regimes in both spatial and temporal scales. We note that Batchelor first discussed mean-square separation by using $\langle\mathbf{r}^2(t)\rangle - \mathbf{r}_0^2$ rather than $\langle|\mathbf{r}(t)-\mathbf{r}_0|^2\rangle$ [6]. In Fig. 5(b) we plot several data sets with $r_0 = 0.9, 1.3, 1.7$, 2.2, and 4.3η using the original definition for pair dispersion $\langle\mathbf{r}^2(t)\rangle - \mathbf{r}_0^2$ [again normalized by $f(r_0)t^2$]. It is seen that the height of these curves shifted downward systematically with increasing r_0. As $\langle r^2(t)\rangle = r_0^2\exp[0.42(t/\tau_\eta)]$ for small values of t and r_0, we plot $\{r_0^2\exp[0.42(t/\tau_\eta)] - r_0^2\}/f(r_0)t^2$ as the dashed red line in the same figure. It is seen that even in the high-resolution compensated plot the symbols agree excellently with the line. Note that the Taylor expansion of $r_0^2\exp[0.42(t/\tau_\eta)] - r_0^2$ with respect to time is dominated by $0.42r_0^2t/\tau_\eta$ for $t/\tau_\eta < 1$. This can explain why the curves for small r_0 tilted up in the dissipative time range for mean-square separations compensated by t^2. Figure 5(b) thus demonstrates the crossover from the exponential to the Batchelor regimes both spatially (when r_0 varies from the dissipative to the inertial range of scales for fixed $t < \tau_\eta$) and temporally (when t varies from smaller than τ_η to greater than τ_η for a fixed $r_0 < \eta$).

IV. SUMMARY AND CONCLUSIONS

To summarize, we have made an experimental study of particle pair dispersions in buoyancy-driven thermal turbulence. In the dissipative subrange of scales, our results show experimentally for the first time the existence of an exponential growth regime for the pair separation $\langle r^2(t)\rangle$, which also yields the Batchelor constant $B = 0.23 \pm 0.07$. For time t smaller and larger than $t_0[=(r_0^2/\epsilon)^{1/3}]$, respectively, the Batchelor and the Richardson-Obukhov scalings are observed in the measured $\langle|\mathbf{r}(t)-\mathbf{r}_0|^2\rangle$. The measured value of the Richardson constant is $g = 0.10 \pm 0.07$.

ACKNOWLEDGMENTS

We thank S. D. Huang for helping with the experiment and H. Xu for helpful discussions. This work is supported in part by the Research Grants Council (RGC) of Hong Kong under Grant No. CUHK404409 and by the NSFC/RGC Joint Research Scheme under Grant No. N_CUHK462/11.

[1] M. Huber, J. C. McWilliams, and M. Ghil, J. Atmos. Sci. **58**, 2377 (2001).
[2] B. Sawford, Annu. Rev. Fluid Mech. **33**, 289 (2001).
[3] J. P. L. C. Salazar and L. R. Collins, Annu. Rev. Fluid Mech. **41**, 405 (2009).
[4] L. F. Richardson, Proc. R. Soc. London A **110**, 709 (1926).

[5] A. M. Obukhov, Izv. Akad. Nauk SSSR, Ser. Geogr. Geofiz. **5**, 453 (1941).
[6] G. K. Batchelor, Q. J. R. Meteorol. Soc. **76**, 133 (1950).
[7] G. K. Batchelor, Proc. R. Soc. London A **213**, 349 (1952).
[8] N. T. Ouellette, H. Xu, M. Bourgoin, and E. Bodenschatz, New J. Phys. **8**, 102 (2006).
[9] S. Ott and J. Mann, J. Fluid Mech. **422**, 207 (2000).
[10] R. Ni, S. D. Huang, and K. Q. Xia, J. Fluid Mech. **692**, 395 (2012).
[11] R. Ni, S.-D. Huang, and K.-Q. Xia, Phys. Rev. Lett. **107**, 174503 (2011).
[12] G. Ahlers, S. Grossmann, and D. Lohse, Rev. Mod. Phys. **81**, 503 (2009).
[13] D. Lohse and K.-Q. Xia, Annu. Rev. Fluid Mech. **42**, 335 (2010).
[14] G. K. Batchelor and A. A. Townsend, in *Surveys in Mechanics*, edited by G. K. Batchelor and R. M. Davies (Cambridge University Press, 1956), pp. 352–399.
[15] S. S. Girimaji and S. B. Pope, J. Fluid Mech. **220**, 427 (1990).
[16] J. Chun, D. L. Koch, S. Rani, A. Ahluwalia, and L. R. Collins, J. Fluid Mech. **536**, 219 (2005).
[17] M. Bourgoin, N. Ouellette, H. Xu, J. Berg, and E. Bodenschatz, Science **311**, 835 (1998).
[18] J. Schumacher, Phys. Rev. E **79**, 056301 (2009).
[19] G. Boffetta and I. M. Sokolov, Phys. Rev. Lett. **88**, 094501 (2002).
[20] P. K. Yeung and M. S. Borgas, J. Fluid Mech. **503**, 93 (2004).
[21] L. Biferale, G. Boffetta, A. Celani, B. J. Devenish, A. Lanotte, and F. Toschi, Phys. Fluids **17**, 115101 (2005).
[22] B. L. Sawford, P. K. Yeung, and J. F. Hackl, Phy. Fluids **20**, 065111 (2008).
[23] J. Schumacher, Phys. Rev. Lett. **100**, 134502 (2008).
[24] R. Ni and K.-Q. Xia, Phys. Rev. E **87**, 023002 (2013).